

Glycans as Biofunctional Ligands for Gold Nanorods: Stability and Targeting in Protein-Rich Media

Isabel García,^{†,‡} Ana Sánchez-Iglesias,[†] Malou Henriksen-Lacey,[†] Marek Grzelczak,^{†,§} Soledad Penadés,^{*,†,‡} and Luis M. Liz-Marzán^{*,†,‡,§}

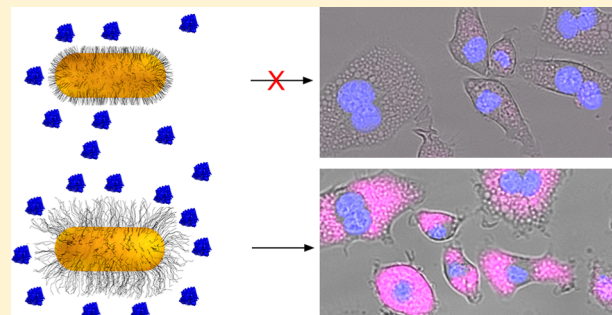
[†]CIC biomaGUNE, Paseo de Miramón 182, 20009 Donostia-San Sebastián, Spain

[‡]Biomedical Research Networking Center in Bioengineering Biomaterials and Nanomedicine (CIBER-BBN), 50018 Aragón, Spain

[§]Ikerbasque, Basque Foundation for Science, 48013 Bilbao, Spain

S Supporting Information

ABSTRACT: Poly(ethylene glycol) (PEG) has become the gold standard for stabilization of plasmonic nanoparticles (NPs) in biofluids, because it prevents aggregation while minimizing unspecific interactions with proteins. Application of Au NPs in biological environments requires the use of ligands that can target selected receptors, even in the presence of protein-rich media. We demonstrate here the stabilizing effect of low-molecular-weight glycans on both spherical and rod-like plasmonic NPs under physiological conditions, as bench-marked against the well-established PEG ligands. Glycan-coated NPs are resistant to adsorption of proteins from serum-containing media and avoid phagocytosis by macrophage-like cells, but retain selectivity toward carbohydrate-binding proteins in protein-rich biological media. These results open the way toward the design of efficient therapeutic/diagnostic glycan-decorated plasmonic nanotools for specific biological applications.



INTRODUCTION

Owing to their unique optical properties, plasmonic nanoparticles (NPs) are promising nanomaterials for theranostics.^{1,2} During the past decade, a number of outstanding works emerged regarding *in vitro* and *in vivo* applications of plasmonic NPs.^{3,4} Hyperthermia,^{5,6} drug delivery,⁷ and bioimaging^{2,8} are only some of the research areas in which plasmonic NPs can be applied. Whereas the physical properties of NPs have been widely demonstrated to be beneficial for biomedical applications, both their chemical stability in biological complex media and the chemical composition of the metal–biofluid interface are also highly relevant.^{9,10} Uncontrolled aggregation of NPs in biological media is usually avoided by decorating them with bulky, close-to-neutral ligands. Important consequences related to cytotoxicity and multiple cellular responses can take place if aggregation occurs in cell culture media or other biological environments.^{11,12} Poly(ethylene glycol) (PEG) has been used as a universal coating for many types of NPs, thus rendering it the obvious gold standard for stabilization of plasmonic NPs toward biological applications. The availability of thiol-terminated PEG largely facilitates postsynthetic functionalization of metal NPs by means of convenient and reproducible protocols. Apart from providing excellent colloidal stability in physiological media,¹³ PEG possesses a highly flexible chain that can adopt a wide variety of conformations, thereby preventing undesired interactions with proteins or other blood components. However, PEG is a synthetic macromolecule, and

as such it also has some drawbacks, such as immunogenic activity.¹⁴ In addition, to effectively stabilize NPs—especially anisotropic ones—in physiological media, PEG with a molar mass of around 5 kD is typically required, which considerably enlarges the overall diameter of the NPs. Bulky PEG ligands often alter the mobility of the NPs, and only passive targeting at the diseased cell/tissues may be achieved with PEGylated NPs. Peptides,¹⁵ polymers,¹⁶ and cationic thiolated ligands,¹⁷ among others,¹⁸ have been used as alternatives to PEG for stabilizing gold nanorods (AuNRs). Nevertheless, the use of short, low-molecular-weight ligands that can ensure colloidal stability, biocompatibility, and targeting properties of plasmonic NPs with different shapes remains an important experimental challenge.

Carbohydrates (glycans or saccharides) are important biomolecules that can selectively bind to clinically relevant proteins and therefore are essential components in inter- and intracellular signaling processes.¹⁹ Biocompatible, non-plasmonic gold nanoparticles (AuNPs, size <3 nm) coated with thiol-terminated glycans (glyconanoparticles) have been widely reported, mainly toward exploiting the multivalent presentation of carbohydrates to address different biological problems.²⁰ Plasmonic spherical gold glyconanoparticles have also been prepared for the study of carbohydrate interactions.^{21,22} These

Received: January 29, 2015

Published: February 23, 2015

glyconanoparticles have been shown to selectively target specific receptors which depend on the attached glycans. However, an important question that still has to be answered is whether the NPs keep their selectivity in the presence of protein-rich media such as serum or whole blood. When placed in a complex biological medium, molecules on the surface of NPs can lose their ability to bind to the targeted receptors on cells because of the formation of the so-called protein corona. It has been recently demonstrated that the ability of transferrin-conjugated NPs to target the receptors was significantly affected after interaction of NPs with serum proteins.²³

We propose here the use of carbohydrates as an alternative to PEG, to stabilize as well as to ensure biocompatibility and targeting capability to anisotropic AuNPs—AuNRs. We expect that the selectivity of glycans toward specific cell types, through targeting carbohydrate-binding receptors (active targeting), will be maintained even in protein-rich media. Functionalization of AuNRs with low-molecular-weight (as compared to PEG) glycans not only ensures colloidal stability in protein-rich physiological media but also prevents phagocytosis by macrophages and exhibits excellent selectivity toward carbohydrate-binding proteins (lectins) in serum and in *in vitro* cultured cells.

■ RESULTS AND DISCUSSION

Gold nanorods stabilized by thiol-terminated glycoconjugates of *N*-acetylglucosamine (GlcNAc) or the disaccharide lactose (Lac) were prepared starting from CTAB-stabilized NRs^{24,25} (length, 64.1 ± 6.6 nm; width, 16.4 ± 1.6 nm; aspect ratio, 3.9 ± 0.4). Additionally, citrate-stabilized nanospheres²⁶ (14.3 ± 1.4 nm, denoted as Au₁₄) were coated with the same neoglycoconjugates for the sake of comparison (Figure 1). The stabilizing (GlcNAc and Lac) neoglycoconjugates were prepared by glycosylation of the corresponding sugars with an amphiphilic thiol-terminated tetra(ethylene glycol)-11 aliphatic chain (TEG-C11-SH) linker (Figure 1a) as previously described.²⁷

Synthesis and Colloidal Stability of Glycan-Decorated Gold Nanorods and Au₁₄ Nanoparticles. Ligand exchange was carried out in water using an excess of the corresponding neoglycoconjugate molecules (see details in the Supporting Information (SI)). Both Au₁₄ and AuNRs were functionalized with either GlcNAc or Lac ligands, showing in all cases excellent stability in water (Figure 1b). Small changes in the architecture of the glycan conjugates, however, strongly affected the colloidal stability. For example, AuNRs aggregated in water when the neoglycoconjugate of glucose was used instead of GlcNAc or Lac. Similarly, the nature of the spacer in the neoglycoconjugates was found to affect NP stability, aggregation being observed when either 5- or 11-carbon-atom aliphatic chains (lacking the TEG moiety) were used as spacers. To evaluate the colloidal stability of Au₁₄ and AuNRs in a complex physiological medium, we incubated the NPs with a standard cell culture medium (Dulbecco's modified Eagle's medium, DMEM) supplemented with 10% fetal bovine serum (FBS). Serum is a complex fluid that contains many different proteins, with concentrations up to 0.07 g/mL (see SI), albumin being the majority protein present at concentrations of about 1 mM. After incubation, no changes in the intensity or in the position of the localized surface plasmon resonance (LSPR) bands were observed in the UV-vis-NIR spectra (Figure S1, SI). Accordingly, TEM characterization (not shown) revealed neither morphological changes nor aggregation of the NPs.

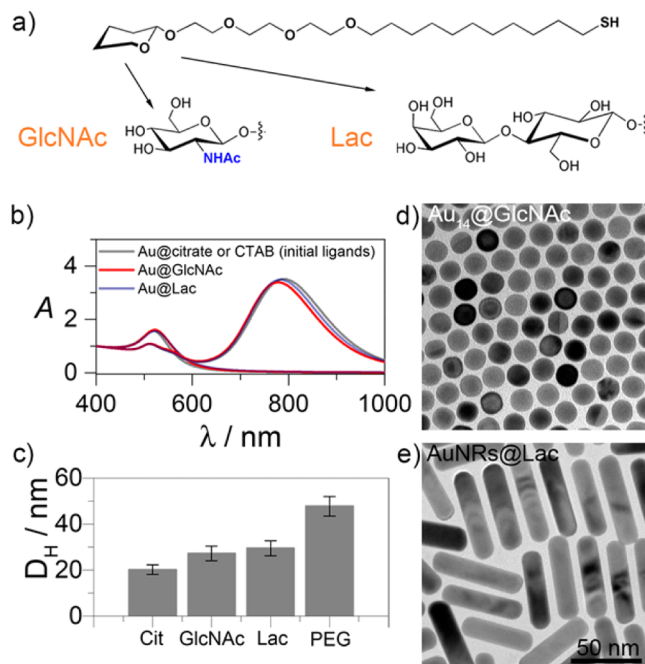


Figure 1. (a) Molecular structures of thiol-terminated neoglycoconjugates of *N*-acetylglucosamine (GlcNAc) and lactose (Lac) used to stabilize gold nanoparticles. (b) UV-vis-NIR spectra of Au₁₄ and AuNRs stabilized with their corresponding glycan and original ligands. (c) Hydrodynamic diameters measured in water for Au₁₄ stabilized with different ligands, as labeled. (d) TEM image of Au₁₄ particles stabilized with GlcNAc. (e) TEM image of AuNRs stabilized with Lac. Similar images were obtained for Au₁₄@Lac and AuNRs@GlcNAc.

As expected, the molecular mass of the ligand molecules does affect the overall diameter of the NPs. The hydrodynamic diameter (D_H) of Au₁₄ protected with the different capping molecules was found to increase from 20 nm for citrate, up to 27 and 30 nm for GlcNAc and Lac, respectively (Figure 1c). Au₁₄ stabilized with PEG (5 kDa) was used as a control sample and yielded, as expected, a larger diameter ($D_H = 49$ nm). Taking into account the relatively short chain length of the carbohydrate neoglycoconjugates and the high stability of the nanostructures in physiological media, carbohydrate ligands appear clearly advantageous over the commonly used PEG.

Assessing Carbohydrate Interaction Specificity. Apart from preventing aggregation, the main advantage of using carbohydrates as stabilizing molecules lies in their molecular affinity toward a number of proteins (lectins) that are involved in a wide variety of cellular functions. To test these targeting properties, we selected two carbohydrate-binding proteins, namely wheat germ agglutinin (WGA) and the β -galactoside-binding lectin galectin-3 (Gal-3), which differ in the binding affinities to their natural ligands. While WGA exhibits affinity toward GlcNAc,²⁸ Gal-3 is selective toward lactose.²⁹ Based on the multivalent character of glycan-lectin interactions,^{22,28b,29b} we explored the selective aggregation of a binary mixture containing AuNPs and AuNRs. We prepared a mixture in water of Au₁₄@Lac and AuNRs@GlcNAc (Figure 2a), so that addition of WGA lectin should lead to selective aggregation of the AuNRs (Figure 2b, left). Indeed, the longitudinal LSPR band of the NRs was observed to blue shift, whereas the LSPR band of spherical NPs remained unchanged, which confirmed the aggregation of AuNRs only (Figure 2c, left). In contrast, addition of Gal-3 to the same binary mixture induced selective

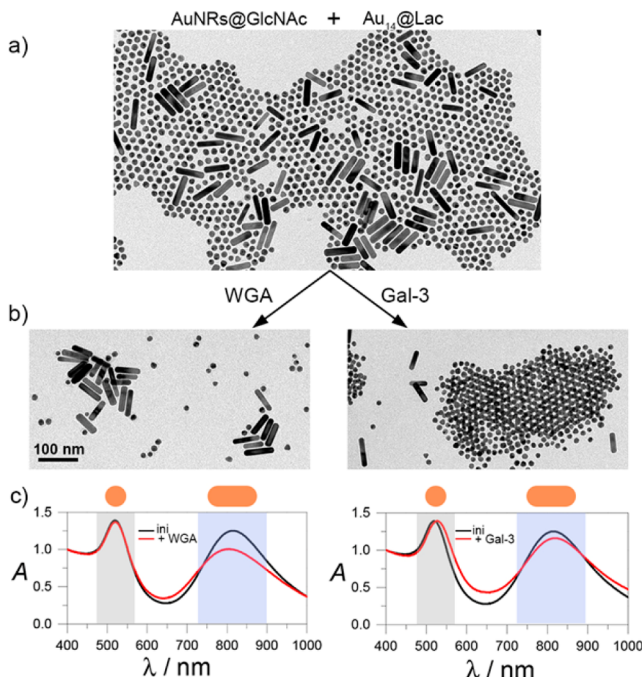


Figure 2. Ligand-driven aggregation of nanoparticles by specific lectins. (a) TEM image of the binary mixture containing AuNRs@GlcNAc and Au₁₄@Lac before addition of proteins (WGA or Gal-3). (b) TEM images of the corresponding binary mixtures after incubation with the different lectins, as indicated. (c) UV-vis-NIR spectra of the binary mixtures before and after protein binding.

aggregation of Au₁₄@Lac (Figure 2b, right). Low-magnification TEM images are shown in Figures S2 and S3 (SI). In this case, the longitudinal LSPR band of AuNRs remained centered at the same wavelength, while that of spherical NPs showed a red shift (~8 nm), indicating aggregation (Figure 2c). Although the particles form extended aggregates, the observed red shift was in fact relatively small, due to the presence of rather large molecules (proteins) separating the particles from each other and hindering efficient plasmon coupling. The selectivity of the glyco-NRs toward lectins shows that the chemical structure of the glycan-stabilizing agent dramatically changes protein–particle interactions and thereby opens new strategies in the fields of self-assembly or biosensing, as previously shown for the assembly of spherical NPs through interactions with lectins.^{30,31}

Binding of Serum Proteins to Nanoparticles. To evaluate whether neoglycoconjugates minimize unspecific interactions of the protected Au₁₄ and AuNRs with other biomolecules present in physiological media, we performed a qualitative comparison between protein adsorption on Au₁₄@GlcNAc and AuNRs@Lac, as well as on PEG-stabilized Au₁₄ and AuNRs as controls. We incubated equal concentrations of NPs (10^{13} particles/mL) with dilute FBS (10% in PBS) for 2 h at 37 °C. The incubated NPs were separated from non-adsorbed proteins by careful centrifugation (4 °C, 6000 rpm for 20 min), followed by extensive and careful washing with PBS to remove all unbound proteins until the supernatant did not contain any detectable protein. Adsorbed proteins were then isolated from the NPs after treatment with sodium dodecyl sulfate (SDS) 10%/dithiothreitol (DTT) 500 mM, and subsequently analyzed by SDS polyacrylamide gel electrophoresis (SDS-PAGE) (Figure 3a) and mass spectrometry (MS) (Table S1, SI). Adequate controls comprised the analysis

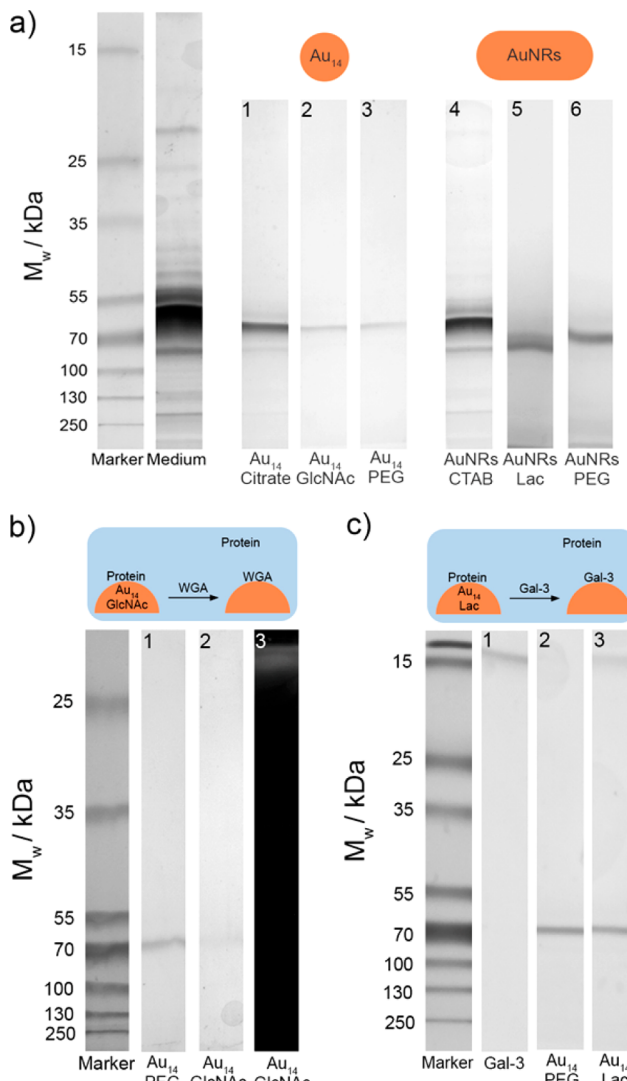


Figure 3. Comparison of proteins immobilized onto the surface of nanoparticles. (a) SDS-PAGE protein binding profiles of Au₁₄ functionalized with citrate, GlcNAc, and PEG5k, and AuNRs stabilized with CTAB, Lac, and PEG5k, exposed to 10% FBS in PBS. The molecular weights of the proteins in the standard marker and an aliquot of FBS (10%) are shown on the left for reference. (b) SDS-PAGE of eluted proteins from Au₁₄@PEG (lane 1) and Au₁₄@GlcNAc (lane 2), and the corresponding fluorescence image (lane 3), precoated with serum proteins (2 h) and subsequently treated with Cy3.3-labeled WGA. Molecular mass is indicated. (c) SDS-PAGE of proteins eluted from Au₁₄@PEG (lane 2) and Au₁₄@Lac (lane 3) exposed to serum proteins (2 h) and subsequently treated with human Gal-3. Molecular mass and an aliquot of human Gal-3 (lane 1) are reported on the left as references.

of all recovered supernatants. The eluted bound proteins from carbohydrate- and PEG-stabilized AuNPs showed no significant differences in banding pattern, displaying band(s) in the range of 55–70 kDa (Figure 3a). The chemical composition of the non-specific protein corona was analyzed by liquid chromatography–tandem mass spectrometry (LC-MS/MS) and was found to be similar to that of the proteins adsorbed on the surfaces of hydrophilic polymeric NPs (Table S1, SI).^{9,10} We also observed that NPs stabilized with anionic (citrate) or cationic (CTAB) ligands adsorb a larger amount of protein than those modified with neutral ligands (PEG and glycans)

(Figure 3a, lanes 1 and 4), thereby reflecting a greater tendency for proteins to bind to charged NPs, which is likely due to electrostatic interactions.^{32,33} In the case of sugar- and PEG-protected NPs, the results indicate that non-specific protein binding depends on the shape of the particles; i.e. AuNRs bind more proteins than spherical Au₁₄ (Figure 3a, lanes 2, 3, 5, and 6). The main reason for such behavior may be the anisotropy of NRs, which has been repeatedly shown to lead to inhomogeneous ligand distributions.³⁴ Since the tips of AuNRs are more reactive than lateral parts, the remaining CTAB molecules on the lateral parts of the rods after ligand exchange may contribute to enhanced protein binding.³⁵ Overall, the low-molecular-weight neoglycoconjugates minimize non-specific interactions with serum proteins in the same extension as PEG5k. A high resistance to protein adsorption onto glycan-decorated plasmonic NPs is thus confirmed.

Impact of Protein Corona on Carbohydrate Targeting.

It is important that sugar molecules preserve their natural targeting specificity in spite of the formation of a protein corona when dispersed in serum. To confirm this, we incubated Au₁₄@GlcNAc and Au₁₄@Lac with FBS (10% in PBS) for 2 h, and then we added Cy3.3 fluorescently labeled WGA and Gal-3, respectively. Treatment of serum-incubated Au₁₄@GlcNAc with excess Cy3.3-labeled WGA led to nearly complete replacement of non-specifically adsorbed serum proteins, as shown by the absence in the corresponding SDS-PAGE gel of a band at ~70 kDa (Figure 3b, lane 2) and the presence of a fluorescent band (Cy3.3-WGA) at ~20 kDa (Figure 3b, lane 3). The addition of Gal-3 to serum-treated Au₁₄@Lac led to only partial serum protein removal, as revealed by SDS-PAGE analysis. The protein corona on Au₁₄@Lac comprises both serum proteins (~70 kDa) and Gal-3 (~15 kDa) (Figure 3c, lane 3). Partial replacement by Gal-3 occurred even though the K_d value for lactose binding to Gal-3 is 35-fold lower than that for free GlcNAc binding to WGA (total replacement).^{28a,29a} This result suggests that, in addition to the affinity of a protein for its ligands, other factors such as multivalent glycan presentation on gold nanoscaffolds or differences in the structural requirements between the selected lectins can affect the composition of adsorbed proteins. SDS-PAGE of proteins eluted from serum-treated Au₁₄@PEG and incubated with WGA and Gal-3 lectins showed only the band corresponding to the protein corona (Figure 3b, lane 1, and Figure 3c, lane 2), whereas no bands corresponding to Cy3.3-labeled WGA and Gal-3 were detected. We can therefore state that the presence of carbohydrates on the AuNPs moderates the negative effect of unspecific protein adsorption and preserves their natural targeting ability, in spite of the protein corona formed in serum.

In Vitro Cell Assays. The unique optical and photothermal properties of AuNRs are particularly attractive for biomedical applications. Therefore, both cytotoxicity and cell-targeting experiments were carried out *in vitro* for glycan-capped AuNRs, so as to evaluate the selectivity of their interactions with different cell lines. To this end, AuNRs@Lac and AuNRs@PEG were labeled with a thiol-terminated dye (HiLyte Fluor647)³⁶ by ligand exchange (details in the Experimental Section). The fluorescently labeled AuNRs emit at 647 nm, in the spectral range between their transverse and longitudinal LSPR modes (Figures S4 and S5, SI). Only a slight difference in fluorescence intensity was observed between the two fluorescently labeled AuNR samples. The presence of lactose on the NRs after fluorescent labeling was confirmed by means of a colorimetric assay with anthrone/sulfuric acid,³⁷ which

yielded a value of 5499 ± 428 lactose molecules per NR, or one lactose molecule per ~ 0.7 nm². The stabilized NRs did not show cytotoxicity at a concentration of 3.5×10^{12} particles/mL (Figure S6, SI).

We selected both a phagocytic macrophage-like cell line (J774) and a colon cancer cell line (DLD1) that express Gal-3 proteins (Figure S7, SI). Since phagocytosis by macrophages is an undesired process for most therapeutic applications of NPs, the ligand coating should act as an invisibility cloak to prevent phagocytosis. On the other hand, Gal-3 is an interesting biomarker because it is involved in a number of biological processes, including apoptosis, cell growth, cell adhesion, cell differentiation, and intracellular trafficking.^{38,39} We first incubated AuNRs stabilized by either PEG or lactose with the macrophage-like cell line J774 at different incubation times (2.5, 4, 6, and 24 h). Figure 4 shows the significantly different

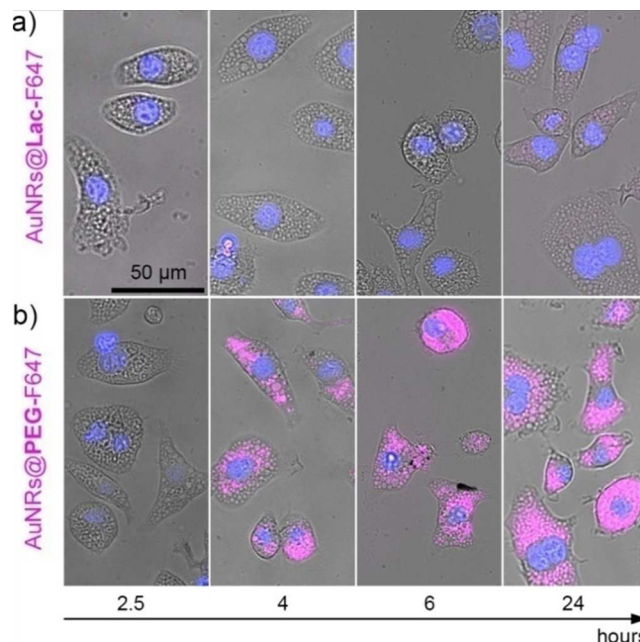


Figure 4. Illustrative examples of the behavior of HiLyte Fluor647-labeled AuNRs@Lac and AuNRs@PEG (AuNRs@Lac-F647 and AuNRs@PEG-F647) internalized by macrophage-like J774 cells over time at 37 °C, 5% CO₂. Fluorescence images of J774 cells incubated with (a) 3×10^5 AuNRs@Lac/mL and (b) 3×10^5 AuNRs@PEG/mL for different times (2.5, 4, 6, and 24 h). The pink color indicates the presence of nanoparticles, whereas blue color denotes the nuclei.

behavior of AuNRs@Lac and AuNRs@PEG toward phagocytosis by J774 macrophages. The level of uptake of AuNRs@Lac was negligible at shorter incubation times (<6 h), but a weak fluorescence emission was observed after 24 h. In contrast, the uptake of AuNRs@PEG was faster, and large amounts of intracellularly taken-up NRs were observed at 24 h, suggesting their presence in phagosomes (Figure 4b).

Finally, we demonstrate that AuNRs@Lac retain their binding specificity for Gal-3 in the cellular environment. Incubation of labeled AuNRs@Lac with DLD-1 cells led to binding of NRs to Gal-3, which can be readily detected by co-localization in fluorescence microscopy images (Figure 5). To quantitatively determine the interaction of the NRs and Gal-3, we performed Pearson's correlation coefficient (PCC) analysis (Figure S8, SI).⁴⁰ The analysis revealed a PCC value of 0.53 ± 0.09 , meaning that there is positive co-localization between Gal-

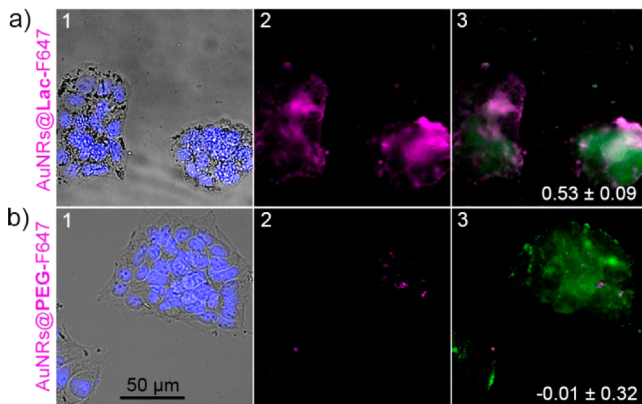


Figure 5. Fluorescence images of DLD1 cells incubated with (a) AuNRs@Lac-F647 (pink) and (b) AuNRs@PEG-F647 and specifically co-stained with anti-human Gal-3 and anti-rabbit IgG secondary antibody (AF488; green) and DAPI (blue) for nuclei. The images are overlays of bright-field and DAPI (1), fluorescence of internalized AuNRs-F647 (2), and AuNRs-F647 and Gal-3 protein staining (AF488) (3). Numbers in white give the value of co-localization analyzed using Pearson's correlation coefficient, ranging from -1 (inverse correlation) to $+1$ (positive correlation). Fluorescence images and PCC values confirm that lactose-conjugated nanoparticles colocalize with Gal-3 in DLD-1 cells. An example of the calculation of PCC is shown in Figure S8 in the Supporting Information. Mean \pm SD values are indicated for both cases. Scale bars are $50\text{ }\mu\text{m}$.

3 and NPs (Figure 5a). As a control we used labeled AuNRs@PEG, which clearly yielded a lack of co-localization ($\text{PCC} = -0.01 \pm 0.32$, Figure 5b). It is worth mentioning that cellular uptake of NPs was studied in a medium supplemented with 5–10% FBS, thereby highlighting the specificity of the interaction between lactose and Gal-3. The targeting property of the glycan-protected nanostructures is thus an important feature that can be exploited in the field of targeted drug delivery and photothermal therapy in complex biological media.

CONCLUSIONS

This study demonstrates that low-molecular-weight glycans not only ensure high colloidal stability and biocompatibility to anisotropic gold nanoparticles but also maintain targeting functionality in protein-rich physiological media. The carbohydrate shell on the surface of plasmonic nanoparticles affords lectin targeting on tumoral cells while avoiding phagocytosis by macrophage-like cells. Given that mammalian lectins play an important role in a number of biological processes (innate immunity, leukocyte trafficking, modulation of cell–cell interactions, cell growth, etc.),⁴¹ our results support the idea that structures of complex and antigenic glycans on plasmonic, anisotropic nanoparticles are suitable candidates for photothermal therapy on highly metastatic tumor cells, for instance, by blocking Gal-3 downstream biological processes.

EXPERIMENTAL SECTION

Materials and Methods. Tetrachloroauric acid (HAuCl_4), trisodium citrate, hexadecyltrimethylammonium bromide (CTAB), silver nitrate (AgNO_3), hydrochloric acid (HCl), ascorbic acid, and O -[2-(3-mercaptopropionylamino)ethyl]- O' -methylpoly(ethylene glycol) 5 kDa (PEG) were purchased from Sigma-Aldrich. Wheat germ agglutinin 36 kDa (WGA) and the β -galactoside-binding lectin galectin-3 (Gal-3) were purchased from Abcam. Dialysis membranes with a molecular weight cut-off (MWCO) of 100 kDa (cellulose ester) and ultrafiltration membranes (regenerated cellulose) were purchased

from Millipore. Milli-Q H_2O (Millipore, Billerica, MA, USA) was used as the solvent. J774 macrophages were purchased from the American Type Culture Collection (ATCC) and were cultured in DMEM supplemented with 5% FBS and 1% penicillin–streptomycin. DLD-1 colorectal adenocarcinoma cells were obtained from ATCC and were grown in Roswell Park Memorial Institute medium supplemented with 10% FBS. Cells were maintained in a humidified atmosphere at $37\text{ }^\circ\text{C}$, 5% CO_2 and passaged by pipetting (J774) or trypsin-EDTA (DLD-1). All reagents were purchased from Invitrogen. UV-vis spectra were measured on a Beckman Coulter DU 800 spectrometer. High-resolution mass spectra (HR-MS) were obtained using the matrix-assisted laser desorption/ionization (MALDI) technique with a 4700 proteomics analyzer (Applied Biosystems) with MALDI-time-of-flight (TOF) configuration. TEM analysis was carried out on a Philips JEOL JEM-2100F instrument working at 200 kV. House-distilled water was further purified using a Milli-Q reagent-grade water system (Millipore). The neoglycoconjugates of lactose (β -D-galactopyranosyl-(1–4)-D-glucose (Lac) and *N*-acetyl-D-glucosamine (GlcNAc) were synthesized as described previously.²⁷

Synthesis of Au₁₄. AuNPs (14 nm) were prepared according to the standard Turkevich method.⁴² HAuCl_4 (50 mM, 5 mL) was added into a boiling aqueous solution of sodium citrate (1.7 mM, 500 mL). After 15 min the reaction was cooled to room temperature.

Synthesis of Gold Nanorods. AuNRs (64 nm \times 16 nm) were synthesized following the seeded growth method.⁴³ Seeds were prepared by reduction of HAuCl_4 (0.25 mM, 5 mL) with NaBH_4 (10 mM, 0.3 mL) in aqueous CTAB solution (100 mM). An aliquot of seed solution (0.6 mL) was added to a growth solution (250 mL) containing CTAB (100 mM), HAuCl_4 (0.5 mM), ascorbic acid (0.8 mM), AgNO_3 (0.12 mM), and HCl (19 mM). The mixture was left undisturbed at $30\text{ }^\circ\text{C}$ for 2 h. The solution was centrifuged twice (8000 rpm, 30 min) to remove excess silver salt, ascorbic acid, CTAB, and HCl and redispersed in Milli-Q water to obtain a final concentration of gold equal to 0.5 mM.

Functionalization of Gold Nanoparticles with Thiol-Terminated PEG and Neoglycoconjugates. An aqueous solution (2 mL) containing 50 molecules/ nm^2 of thiol-terminated PEG or thiol-terminated carbohydrates (GlcNAc and Lac, 7.69×10^{-6} mol for 14 nm nanospheres and 5.95×10^{-6} mol for AuNRs) was added dropwise under vigorous stirring to as-synthesized gold nanospheres or to washed (see above) AuNRs (50 mL, $[\text{Au}] = 0.5\text{ mM}$). The mixture was allowed to react for 2 h. PEG and carbohydrate-modified particles were then centrifuged twice to remove excess carbohydrate and redispersed in 2 mL of water.

Analysis of Serum Protein Binding by SDS-PAGE and LC-MS/MS. Equal quantities of each type of AuNPs (10^{12} particles, 10^{13} particles/mL) were added to FBS diluted in PBS to reach a final serum protein concentration of 10% v/v (equal to that present in the *in vitro* cell experiments) and incubated for 2 h at $37\text{ }^\circ\text{C}$. After incubation, protein corona/AuNP complexes were isolated by centrifugation at $4\text{ }^\circ\text{C}$, 6000 rpm for 20 min. This standard washing procedure was repeated several times until no protein detection was observed in the washings by the Bradford method before the final pellet was resuspended in 50 μL of PBS. Bound proteins were isolated by adding SDS (10%, 25 μL)/DTT (500 mM, 25 μL)⁴⁴ and incubating 1 h at $70\text{ }^\circ\text{C}$. After a final centrifugation at $4\text{ }^\circ\text{C}$, 13000g for 2 min, equal-volume aliquots were loaded and resolved on 12% acrylamide SDS-PAGE, run for \sim 50 min, and stained with Coomassie or with silver stain. Gels were scanned using a Bio-Rad GS-800 calibrated densitometry scanner. For protein identification by MS, bands of interest from SDS-PAGE gels (12%) were excised and digested in gel with trypsin according to the method of Shevchenko et al.⁴⁵ with minor variations. The resulting peptide mixtures were resuspended in 0.1% formic acid and analyzed by electrospray LC-MS/MS. For a complete description of LC-MS/MS, see SI.

Selective Aggregation of AuNRs from Binary Mixtures. To a binary solution (2 mL, water) containing $\text{Au}_{14}\text{@Lact}$ (2×10^{-7} mol in terms of atomic Au) and AuNRs@GlcNAc (1×10^{-7} mol) was added a WGA solution (0.1 mL in PBS 10 mM, 7.8×10^{-4} mM) under

gentle magnetic stirring. The solution was left undisturbed at 37 °C for 12 h.

Selective Aggregation of Au₁₄ from Binary Mixtures. To induce selective aggregation of Au₁₄@Lac by Gal-3, the protein needs to be first activated by lactose in 5:1 molar ratio.²⁹ Gal-3 (10 µg) was solubilized in an aliquot of lactose aqueous solution (3 µL, 0.026 mM) and diluted with water to a final volume of 77 µL. The final concentration of Gal 3 was 5 × 10⁻³ mM. Gal-3 solution (7.4 µL, 5.10⁻³ mM) was then added to the binary mixture (2 mL) containing Au₁₄@Lact (2 × 10⁻⁷ mol in terms of atomic Au) and AuNRs@GlcNAc (1 × 10⁻⁷ mol) under gentle magnetic stirring. The solution was left undisturbed at 37 °C for 12 h and afterward analyzed.

HiLyte Fluor647 Dye Conjugation to PEG and Lactose AuNRs. HiLyte Fluor647, with a thiol-terminated amphiphilic linker, was prepared according to a reported procedure.³⁶ HiLyte Fluor647 thiol-ending conjugate (1 µL, 0.00175 µmol) was incubated with 1.5 × 10¹³ particles of AuNR@PEG or AuNR@Lac and stirred at 1000 rpm at 25 °C. After 2 h of incubation, the AuNRs were diluted to 1 mL with water and filtered by using an Amicon Ultra centrifugal filter (100 000 MWCO, Millipore) in a Heraeus Megafuge 16R centrifuge (Thermo Scientific) at 18 °C and 3000g until a free dye-containing filtrate was obtained. Finally, the fluorescently labeled AuNRs, AuNRs@PEG-F647 and AuNRs@Lac-F647, were resuspended in 100 µL of PBS (pH 7.4, 10 mM) and kept in the dark at 4 °C until further use. This protocol was performed, as far as possible, in the absence of light.

Determination of Carbohydrate Density on Nanoparticles. A freshly prepared anthrone solution in concentrated H₂SO₄ (0.5 wt %, 1 mL) was added to various concentrations of lactose neoglycoconjugate in water (0.3 mL) in an ice bath under stirring. Solutions were heated at 100 °C during 10 min. After the solutions cooled to room temperature, their absorbance at 620 nm was measured, and the data were plotted against the concentration of lactose. These measurements were used as a calibration curve for the calculation of the ligand density on AuNRs@Lac. Lactose density determination for AuNRs@Lac-F647 was carried out by dissolving the NRs (10 µL, 6.36 × 10¹² particles/mL) in 100 µL of Milli-Q water, adding anthrone/H₂SO₄, and following the above protocol. The final data were the mean values of three measurements with less than 5% variation. AuNRs@PEG-F647 was also evaluated with anthrone/H₂SO₄ treatment, and the absorbance at 620 nm was used as the background deducted from the total signals measured from the AuNRs@Lac-F647. The density of lactose immobilized was then determined using the calibration curve.

Cell Uptake of Nanoparticles. Cells were detached from growth flasks, counted, and plated in six-well µ-slides (Ibidi) at a concentration of 3 × 10⁵ cells/mL, 30 µL/well. After attachment overnight, DMEM was removed from the reservoirs, taking care to not allow bubbles to enter in the channel. The F647-labeled NRs were diluted in media to a concentration of 5 × 10¹⁰ particles, and a 100 µL aliquot was added per channel. As a control, an equivalent volume of water diluted in medium instead of NRs was added to cells. Cells were left for 24 h at 37 °C.

Staining of Gal-3 in Cells. Medium in channels was replaced with formaldehyde (4% in PBS) and left for 15 min at room temperature and pressure. Cells were washed twice with ice-cold PBS, followed by incubation in PBS with Triton X100 (0.25%) for 10 min. Cells were washed three times in PBS for 5 min each. A 1% solution of BSA (Sigma) in PBST (10 mM PBS with 0.1% Tween20) was added, and cells were incubated for 30 min at 37 °C. Without washing, rabbit polyclonal anti-galactin 3 antibody in PBST (1/500) (Abcam, Cambridge) was added for 1 h at 37 °C. Cells were washed three times with ice-cold PBS, followed by incubation for 1 h with donkey anti-rabbit (AF488) IgG secondary antibody (1/500 in PBS including 1% BSA) (Abcam). After three additional washes with PBS, cells were stained with DAPI (1/1000 in cell media) (Invitrogen) and left in PBS for microscopy.

Fluorescence Microscopy Analysis. Samples were viewed using a Zeiss Axio Observer microscope with the following setup: 365 nm LED for excitation of DAPI, 470 nm LED for excitation of AF488 (Gal-3), 590 nm LED for excitation of HiLyte Fluor647 (nano-

particles) and transmitted light. Images were taken using a 20× air objective (0.8NA). Exposure times for nanoparticles were kept constant for all samples; exposure times of Dapi and AF488 were altered according to cell type and Gal-3 expression. Multi-acquisition images were taken, and AF488 and AF647 channels were selected for co-localization analysis.

ASSOCIATED CONTENT

S Supporting Information

Supplementary figures, tables, synthetic schemes, experimental procedures, and additional characterization of AuNPs. This material is available free of charge via the Internet at <http://pubs.acs.org>.

AUTHOR INFORMATION

Corresponding Authors

*spenades@cicbiomagune.es

*llizmarzan@cicbiomagune.es

Notes

The authors declare no competing financial interest.

ACKNOWLEDGMENTS

The proteomic analysis was performed in the proteomics platform at CIC bioGUNE that belongs to ProteoRed, PRB2-ISCIII, supported by grant PT13/0001. This work has been supported by the Spanish MINECO (CT2011-27268 and MAT2013-46101-R) and the Basque Department of Economical Development and Competitiveness (ETORTEK IE13-371).

REFERENCES

- (1) Grzelczak, M.; Perez-Juste, J.; Mulvaney, P.; Liz-Marzán, L. M. *Chem. Soc. Rev.* **2008**, *37*, 1783–1791.
- (2) Dreaden, E. C.; Alkilany, A. M.; Huang, X.; Murphy, C. J.; El-Sayed, M. A. *Chem. Soc. Rev.* **2012**, *41*, 2740–2779.
- (3) Dykman, L.; Khletsov, N. *Chem. Soc. Rev.* **2012**, *41*, 2256–2282.
- (4) Cao-Milán, R.; Liz-Marzán, L. M. *Exp. Opin. Drug Delivery* **2014**, *11*, 741–752.
- (5) Cherukuri, P.; Glazer, E. S.; Curley, S. A. *Adv. Drug Delivery Rev.* **2010**, *62*, 339–345.
- (6) Arvizo, R. R.; Bhattacharyya, S.; Kudgus, R. A.; Giri, K.; Bhattacharyya, R.; Mukherjee, P. *Chem. Soc. Rev.* **2012**, *41*, 2943–2970.
- (7) Ghosh, P.; Han, G.; De, M.; Kim, C. J.; Rotello, V. M. *Adv. Drug Delivery Rev.* **2008**, *60*, 1307–1315.
- (8) Mieszkowska, A. J.; Mulder, W. J. M.; Fayad, Z. A.; Cormode, D. P. *Mol. Pharmaceutics* **2013**, *10*, 831–847.
- (9) Monopoli, M. P.; Aberg, C.; Salvati, A.; Dawson, K. A. *Nat. Nanotechnol.* **2012**, *7*, 779–786.
- (10) Fleischer, C. C.; Payne, C. K. *Acc. Chem. Res.* **2014**, *47*, 2651–2659.
- (11) Liu, X.; Chen, Y.; Li, H.; Huang, N.; Jin, Q.; Ren, K.; Ji, J. *ACS Nano* **2013**, *7*, 6244–6257.
- (12) Cho, E. C.; Zhang, Q.; Xia, Y. *Nat. Nanotechnol.* **2011**, *6*, 385–391.
- (13) Jokerst, J. V.; Lobovkina, T.; Zare, R. N.; Gambhir, S. S. *Nanomedicine* **2011**, *6*, 715–728.
- (14) Knop, K.; Hoogenboom, R.; Fischer, D.; Schuber, U. S. *Angew. Chem., Int. Ed.* **2010**, *49*, 6288–6308.
- (15) (a) Oyelere, A. K.; Chen, P. C.; Huang, X.; El-Sayed, I. H.; El-Sayed, M. A. *Bioconj. Chem.* **2007**, *18*, 1490–1497. (b) Adura, C.; Guerrero, S.; Salas, E.; Medel, L.; Riveros, A.; Mena, J.; Arbiol, J.; Albericio, F.; Giralt, E.; Kogan, M. J. *ACS Appl. Mater. Interfaces* **2013**, *5*, 4076–4085.
- (16) (a) Nie, Z.; Fava, D.; Kumacheva, E.; Zou, S.; Walker, G. C.; Rubinstein, M. *Nat. Mater.* **2007**, *6*, 609–614. (b) Kinnear, C.;

- Burnand, D.; Clift, M. J. D.; Kilbinger, A. F. M.; Rothen-Rutishauser, B.; Petri-Fink, A. *Angew. Chem., Int. Ed.* **2014**, *53*, 12613–12617.
- (17) Vigderman, L.; Manna, P.; Zubarev, E. R. *Angew. Chem., Int. Ed.* **2012**, *51*, 636–641.
- (18) Alkilany, A. M.; Thompson, L. B.; Boulos, S. P.; Sisco, P. N.; Murphy, C. J. *Adv. Drug Delivery Rev.* **2012**, *64*, 190–199 and references therein.
- (19) *Essentials of Glycobiology*, 2nd ed.; Cold Spring Harbor Laboratory Press: Cold Spring Harbor, NY, 2009.
- (20) (a) de La Fuente, J. M.; Barrientos, A. G.; Rojas, T. C.; Rojo, J.; Cañada, J.; Fernández, A.; Penadés, S. *Angew. Chem., Int. Ed.* **2001**, *40*, 2257–2261. (b) Marradi, M.; Martin-Lomas, M.; Penadés, S. *Adv. Carbohydr. Chem. Biochem.* **2010**, *64*, 211–290.
- (21) Reynolds, A. J.; Haines, A. H.; Russell, D. A. *Langmuir* **2006**, *22*, 1156–1163.
- (22) Marradi, M.; Chiodo, F.; García, I.; Penadés, S. *Chem. Soc. Rev.* **2013**, *42*, 4728–4745.
- (23) Salvati, A.; Pitek, A. S.; Monopoli, M. P.; Prapainop, K.; Bombelli, F. B.; Hristov, D. R.; Kelly, P. M.; Aberg, C.; Mahon, E.; Dawson, K. A. *Nat. Nanotechnol.* **2013**, *8*, 137–143.
- (24) Nikoobakht, B.; El-Sayed, M. A. *Chem. Mater.* **2003**, *15*, 1957–1962.
- (25) Sau, T. P.; Murphy, C. J. *Langmuir* **2004**, *20*, 6414–6420.
- (26) Turkevich, J. *Gold Bull.* **1985**, *18*, 125–131.
- (27) Barrientos, A. G.; de la Fuente, J. M.; Rojas, T. C.; Fernandez, A.; Penadés, S. *Chem.—Eur. J.* **2003**, *9*, 1909–1921.
- (28) (a) Neurohr, K. J.; Lacelle, N.; Mantsch, H. H.; Smith, I. C. *Biophys. J.* **1980**, *32*, 931–938. (b) Schwefel, D.; Maierhofer, C.; Beck, J. G.; Seeberger, S.; Diederichs, K.; Möller, H. M.; Welte, W.; Wittmann, V. *J. Am. Chem. Soc.* **2010**, *132*, 8704–8719.
- (29) (a) Saraboji, K.; Håkansson, M.; Genheden, S.; Diehl, C.; Qvist, J.; Weininger, U.; Nilsson, U. J.; Leffler, H.; Ryde, U.; Akke, M.; Logan, D. T. *Biochemistry* **2012**, *51*, 296–306. (b) Lepur, A.; Salomonsson, E.; Nilsson, U. J.; Leffler, H. *J. Biol. Chem.* **2012**, *287*, 21751–21756.
- (30) Craig, D.; Simpson, J.; Faulds, K.; Graham, D. *Chem. Commun.* **2013**, *49*, 30–32.
- (31) Ding, L.; Qian, R.; Xue, Y.; Cheng, W.; Ju, H. *Anal. Chem.* **2010**, *82*, 5804–5809.
- (32) Cedervall, T.; Lynch, I.; Lindman, S.; Berggard, T.; Thulin, E.; Nilsson, H.; Dawson, K. A.; Linse, S. *Proc. Natl. Acad. Sci. U.S.A.* **2007**, *104*, 2050–2055.
- (33) Gessner, A.; Lieske, A.; Paulke, B.; Muller, R. *Eur. J. Pharm. Biopharm.* **2002**, *54*, 165–170.
- (34) Kinnear, C.; Dietsch, H.; Clift, M. J.; Endes, C.; Rothen-Rutishauser, B.; Petri-Fink, A. *Angew. Chem., Int. Ed.* **2013**, *52*, 1934–1938.
- (35) Kah, J. C. Y.; Chen, J.; Zubieta, A.; Hamad-Schifferli, K. *ACS Nano* **2012**, *6*, 6730–6740.
- (36) Murray, R. A.; Qiu, Y.; Chiodo, F.; Marradi, M.; Penadés, S.; Moya, S. E. *Small* **2014**, *10*, 2602–2610.
- (37) Nolting, B.; Yu, J. J.; Liu, G. Y.; Cho, S. J.; Kauzlarich, S.; Gervay-Hague, J. *Langmuir* **2003**, *19*, 6465–6473.
- (38) Califice, S.; Castronovo, V.; Van den Brule, F. *Int. J. Oncol.* **2004**, *25*, 983–992.
- (39) Hittelet, A.; Legendre, H.; Nagy, N.; Bronckart, Y.; Pector, J. C.; Salmon, I.; Yeaton, P.; Gabius, H. J.; Kiss, R.; Camby, I. *Int. J. Cancer* **2003**, *103*, 370–379.
- (40) Dunn, K. W.; Kamocka, M. M.; McDonald, H. *Am. J. Physiol. Cell. Physiol.* **2011**, *300*, C723–C742.
- (41) Sharon, N.; Lis, H. *Glycobiology* **2004**, *14*, 53–62.
- (42) Enustun, B. V.; Turkevich, J. *J. Am. Chem. Soc.* **1963**, *85*, 3317–3328.
- (43) Liu, M.; Guyot-Sionnest, P. *J. Phys. Chem. B* **2005**, *109*, 22192–22200.
- (44) Tenzer, S.; Docter, S. D.; Rosfa, S.; Włodarski, A.; Kuharev, J.; Rekik, A.; Knauer, S. K.; Bantz, C.; Nawroth, T.; Bier, C.; Sirirattanapan, J.; Mann, W.; Treuel, L.; Zellner, R.; Maskos, M.; Schild, H.; Stauber, R. H. *ACS Nano* **2011**, *9*, 7155–7167.
- (45) Shevchenko, A.; Wilm, M.; Vorm, O.; Mann, M. *Anal. Chem.* **1996**, *68*, 850–858.